Interference Oscillations in the Angular Distribution of Laser-Ionized Electrons near Ionization Threshold

D. G. Arbó,* S. Yoshida, E. Persson, K. I. Dimitriou,† and J. Burgdörfer

Institute for Theoretical Physics, Vienna University of Technology, Wiedner Hauptstraße 8-10/136, A-1040 Vienna, Austria, EU

(Received 6 July 2005; published 13 April 2006)

We analyze the two-dimensional momentum distribution of electrons ionized by few-cycle laser pulses in the transition regime from multiphoton absorption to tunneling by solving the time-dependent Schrödinger equation and by a classical-trajectory Monte-Carlo simulation with tunneling (CTMC-T). We find a complex two-dimensional interference pattern that resembles above threshold ionization (ATI) rings at higher energies and displays Ramsauer-Townsend-type diffraction oscillations in the angular distribution near threshold. CTMC-T calculations provide a semiclassical explanation for the dominance of selected partial waves. While the present calculation pertains to hydrogen, we find surprising qualitative agreement with recent experimental data for rare gases [A. Rudenko *et al.*, J. Phys. B **37**, L407 (2004)].

DOI: 10.1103/PhysRevLett.96.143003 PACS numbers: 32.80.Rm, 03.65.Sq, 32.80.Fb

The interaction of few-cycle laser pulses with matter has recently attracted considerable interest [1] as increasingly shorter pulses with duration of the order of 10 fs and below became available. Novel aspects of laser-matter interactions such as the dependence of high-harmonic radiation or electron emission on the carrier envelope phase [2,3] and the interference of electronic wave packets emitted at different points in time during the ultrashort pulse [4] became apparent. Another recent advance is the imaging of the momentum distribution of the ionized electron providing insight into the ejection of both one-electron [5] and nonsequential multiple electron emission [6]. For single-electron emission, the longitudinal momentum distribution (k_z along the direction of the laser polarization) of photoelectrons from rare gases features a broad ''double-hump'' structure near threshold ($E \simeq 0$) which surprisingly resembles the k_z distribution for nonsequential double ionization [7]. While for the latter case this structure results from electron-electron collision during rescattering of the laser-driven electron at the ionic core, in the former case it is due to the interplay of the Coulomb interaction and laser field on the receding trajectory [7–10]. By contrast, the transverse momentum distribution features a narrow Coulomb-like cusp well known from ion-atom collisions [9,11,12]. Very recently, Rudenko *et al.* [5] presented first fully two-dimensional (k_z, k_ρ) momentum maps for laser-ionized electrons from different rare gases, displaying a complex pattern whose origin is, so far, unexplained. A theoretical investigation performed few years ago by de Bohan [13] predicted similar patterns. In this Letter we investigate the 2D momentum map for laser ionization of hydrogen and find an equally complex yet surprisingly similar pattern suggesting a simple explanation, in terms of interferences between different electron trajectories in the combined laser and Coulomb field. The pattern is largely independent of the atomic core potential.

The interaction between the laser field and the atom can be characterized by two different mechanisms controlled by the value of the Keldysh parameter $\gamma = \sqrt{I_p/2U_p}$, where I_p is the ionization potential of the atom, $U_p = F_0^2/4\omega^2$ the ponderomotive energy, ω the laser angular frequency, and F_0 the peak amplitude of the laser field. In the multiphoton regime ($\gamma \gg 1$) the atomic interaction is governed by the quantum nature of the radiation field resulting in the absorption of n photons ($n \geq 1$) from the field. By contrast, in the tunneling regime ($\gamma \ll 1$) the atom responds to the strong perturbation by a ''classical'' electric field where ionization proceeds via tunneling. The present calculation as well as recent experiments [5] explores the transition regime around $\gamma \approx 1$ where a more complex response is to be expected. We focus on hydrogen in order to avoid any ambiguity resulting from additional approximations required for many-electron targets.

The Hamiltonian of a hydrogen atom driven by a linearly polarized laser field is

$$H = \frac{\vec{p}^2}{2} - \frac{1}{r} + zF(t), \tag{1}$$

where $\vec{p}$ and $\vec{r}$ are the momentum and position of the electron, respectively, and $F(t)$ is the time-dependent external field linearly polarized along the $\hat{z}$ direction. The laser pulse is chosen to be of the form

$$F(t) = F_0 \sin^2\left(\frac{\pi t}{\tau}\right)\cos(\omega t) \qquad (0 \leq t \leq \tau), \tag{2}$$

where τ is the total pulse duration and F_0 the peak field. Atomic units are used throughout.

The time-dependent Schrödinger equation (TDSE) can be solved by different techniques [14,15]. Approximation methods include semiclassical approximation methods [16,17], the (Coulomb-)Volkov approximation [18,19], and classical-trajectory Monte-Carlo simulation with tunneling (CTMC-T) method [9,20]. We employ the generalized pseudospectral method for solving the TDSE [21]. The method combines a discretization of the radial coordinate optimized for the Coulomb singularity with quad-

rature methods to allow stable long-time evolution using a split-operator method. Both the unbound as well as the bound parts of the wave function $|\psi(t)\rangle$ can be accurately represented. The calculation of the 2D momentum distribution requires projection of the partial waves $|k, l\rangle$ onto outgoing Coulomb waves

$$\frac{dP}{d\vec{k}} = \frac{1}{4\pi k}\left|\sum_l e^{i\delta_l(k)}\sqrt{2l+1}P_l(\cos\theta_k)\langle k, l|\psi(\tau)\rangle\right|^2, \quad (3)$$

after the conclusion of the pulse. In Eq. (3) $\delta_l(k)$ is the momentum-dependent Coulomb phase shift, θ_k is the angle between $\vec{k}$ and the polarization direction of the laser field, $\hat{z}$, P_l is the Legendre polynomial of degree l, and $|k, l\rangle$ is the eigenstate of the atomic Hamiltonian with positive eigenenergy $E = k^2/2$ and orbital quantum number l. The atom is initially in its ground state. Because of the cylindrical symmetry of our system for a linearly polarized laser field, the magnetic quantum number m is a constant of motion ($m = 0$). The distortion of the momentum distribution due to long-range final-state Coulomb interactions is fully accounted for in Eq. (3). We also have performed classical-trajectory Monte-Carlo calculations [9] incorporating tunneling (CTMC-T) which include both Coulomb and laser field interaction nonperturbatively.

Examples of the two-dimensional momentum distribution (k_ρ, k_z), $\frac{d^2P}{dk_\rho dk_z} = 2\pi k_\rho(\frac{dP}{d\vec{k}})$, for an 8-cycle pulse ($\tau = 1005$), frequency $\omega = 0.05$, and different field amplitudes $F_0 = 0.0377(\gamma = 1.34)$, $0.0533(\gamma = 0.95)$, and $0.075(\gamma = 0.67)$ are shown in Fig. 1, illustrating the transition from the multiphoton to the tunneling regime. Each frame displays a complex interference pattern which is characterized by a transition from a ring-shaped pattern at larger $k = \sqrt{k_\rho^2 + k_z^2} \gtrsim 0.4$ with circular nodal lines to a pattern of pronounced radial nodal lines for small k near threshold. The first point to be noted is that the overall pattern displays a surprising and striking similarity to the experimental pattern observed recently for rare gases, such as helium, neon, and argon [5]. The ring pattern is reminiscent of above threshold ionization (ATI) peaks of the multiphoton regime. The point to be noticed is that ATI rings are present well into the tunneling regime for energies $E = \frac{1}{2}k^2 \gtrsim \omega$. In Fig. 1(c) the border between the threshold region and the onset of ATI rings is plotted. Concurrent CTMC-T calculations for the present laser parameters show that classical trajectories provide only a minor contribution to the electron spectra above $E = 2U_p$. Since this region is effectively inaccessible by the classical quiver motion, the multiphoton quantum process is the dominant pathway.

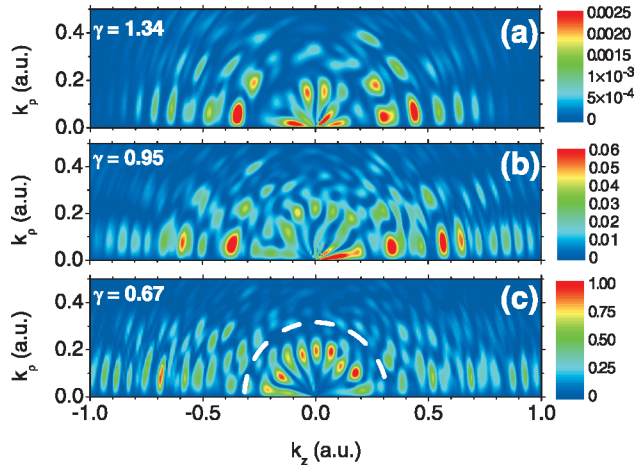

FIG. 1 (color). Doubly differential electron momentum distributions in cylindrical coordinates (k_z, k_ρ). The parameters of the field are $\omega = 0.05$, $\tau = 1005$. In (a) $\gamma = 1.34$ ($F_0 = 0.0377$), (b) $\gamma = 0.95$ ($F_0 = 0.053$), and (c) $\gamma = 0.67$ ($F_0 = 0.075$). In (c) the border between the first and second ATI rings is drawn as a dashed line.

The transition to an entirely different and unexpected radial pattern occurs for energies below $\approx\omega$ from the threshold. The radial nodal pattern at low energies can be made more explicit by analyzing the angular differential probability, $d^2P/dkd(\cos\theta_k)$, at fixed k (Fig. 2). The probability displays pronounced oscillations that remarkably resemble those of a single Legendre polynomial,

$$\frac{d^2P}{dkd(\cos\theta_k)} \approx [P_{l_0}(\cos\theta_k)]^2. \quad (4)$$

At low $k = 0.19$ the Legendre polynomial $l_0 = 8$ has the largest weight. The dominance of a single Legendre polynomial P_l implies the dominance of a single partial wave in the momentum-differential ionization cross section. The resulting radial nodal pattern with pronounced minima at certain angles is a well-known feature in low-to-intermediate energy electron-atom scattering referred to as generalized Ramsauer-Townsend (GRT) diffraction oscillations [22–24]. The present result suggests that laser-driven scattering of electrons in the Coulomb field of the nucleus leads to similar Ramsauer-Townsend-like interference fringes in the angular distribution.

The distribution of contributing partial waves, p_l, is presented in Fig. 3. The ATI-like component can be quan-

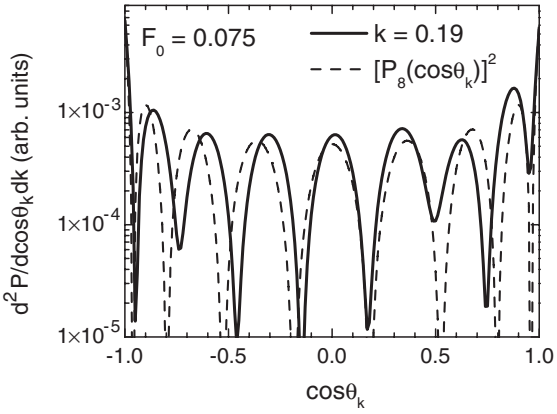

FIG. 2. Angular distribution calculated by solving the TDSE (thick solid lines) for $\omega = 0.05$, $\tau = 1005$, $\gamma = 0.67$ ($F_0 = 0.075$), and $k = 0.19$. Dashed lines: square of the Legendre polynomial $P_{l_0}(\cos\theta_k)$, $l_0 = 8$.

tified by the partial ionization probability p_l^i with orbital quantum number l residing within a given ith ring between adjacent minima $(k_i - \Delta_i, k_i + \Delta_i)$

$$p_l^i = \int_{k_i-\Delta_i}^{k_i+\Delta_i} k dk |\langle k, l|\psi(\tau)\rangle|^2. \quad (5)$$

The ith circle has a mean radius $k_i = \sqrt{2E_i}$, where the energy E_i corresponds to the ith ATI peak of the photoelectron spectrum. For $i \gtrsim 2$ ($k > 0.4$) rings become recognizable. Angular distributions well into the multiphoton regime ($\gamma > 2$) were first presented by Schafer and Kulander [25]. In the tunneling regime ($\gamma = 0.67$, Fig. 3), the partial-wave distribution near threshold peaks at $l_0 = 8$. The dominance of a single l is further enhanced by the relative suppression of adjacent angular momentum $l_0 \pm 1$ of opposite parity, which is a remnant of the multiphoton parity selection rule. The second ring shows a peak at $l_0 = 9$, even though no dominance of a single partial wave is evident when looking at the angular distribution (not shown).

Unlike in the multiphoton regime [25], a simple semiclassical analysis of the interference pattern in the angular distribution can be performed in the tunneling regime (Fig. 3). GRT interference fringes in electron-atom scattering can be semiclassically described in terms of interferences of paths with (in general) different angular momenta scattered into the same angle θ_k [24]. In the special case that a single partial wave and thus a single Legendre polynomial $P_{l_0}(\cos\theta_k)$ dominates, the angular distribution of the interfering paths must have very similar classical ''impact parameters'' such that they belong to the same quantized angular momentum bin $L \in [l_0, l_0 + 1]$. An analogous path interference occurs in laser-atom ionization in the tunneling regime near threshold. To uncover the relevant classical paths we employ a CTMC-T simulation [9] for the same parameters as in Fig. 3. The ensemble of ionized electrons near threshold features, indeed, an L distribution [Fig. 4(a)] that resembles the quantum distribution (Fig. 3) with a peak near $l_0 = 8$, clearly emphasizing the underlying classical character of this process. Moreover, the classical angular distribution [Fig. 4(b)] for trajectories close to threshold ($k \leq 0.26$) confined to the dominant angular momentum bin ($8 \leq L \leq 9$) covers, indeed, all polar angles ($0 \leq \theta_k \leq \pi$) and thus satisfies the requirement for GRT oscillations dominated by a single Legendre polynomial. They correspond to Kepler hyperbolas with very similar opening angles of their asymptotes, but with the angle of major axis relative to the laser polarization distributed between 0 and π. At higher k, the angular distribution becomes much narrower and the dominance of a single partial wave should disappear. A typical electron trajectory after tunneling shows a quiver motion along the polarization of the laser field. An interesting observation is that even though the motion is strongly driven by the laser field, the motion follows the Kepler hyperbola [Fig. 4(c)]. The point to be emphasized is that the dashed line in the Fig. 4(c) does not represent the laser-driven trajectory averaged over a quiver oscillation period but the unperturbed Kepler hyperbola with the identical asymptotic momentum as the laser-driven trajectory (solid line). Thus, the angular momentum of the Kepler hyperbola is identical to that of the asymptotic L of the laser-driven electron. The distance between the hyperbola and the nucleus at the pericenter is given by [26] $r_{\min} = [\sqrt{1 + (kL)^2} - 1]/k^2$. Identifying the pericenter of the hyperbola with the quiver amplitude, $r_{\min} = \alpha$

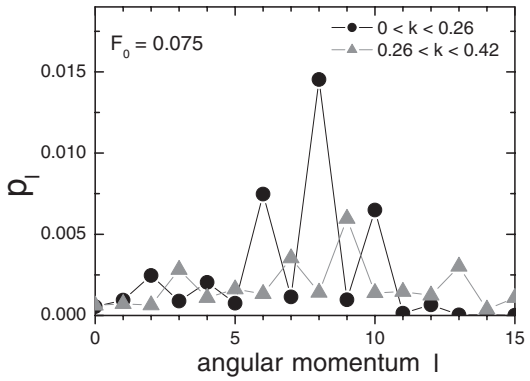

FIG. 3. Partial ionization probability, p_l, as a function of the angular momentum l for different spectral regions indicated in the figure. The parameters of the field are $\omega = 0.05$, $\tau = 1005$, and $\gamma = 0.67$ ($F_0 = 0.075$).

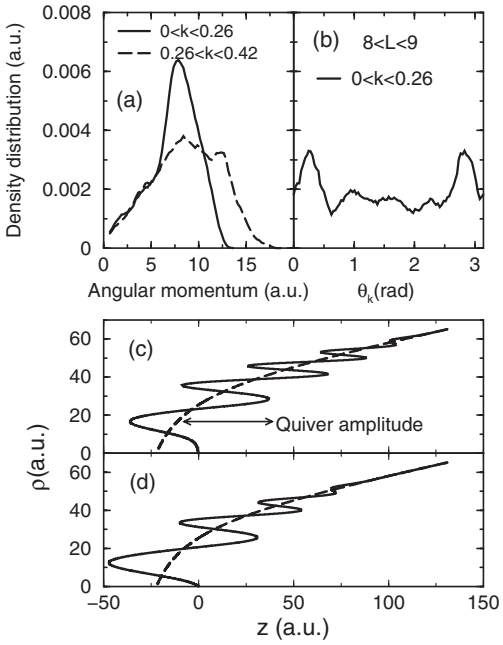

FIG. 4. (a) L distribution of classical trajectories for the same parameters as in Fig. 3. (b) Classical angular distribution for $l = 8$ ($L \in [8, 9]$) in the region $k < 0.26$. (c), (d) Classical trajectories of laser-driven electrons (solid lines) and unperturbed Kepler hyperbola of same asymptotic E and L (dashed lines) differing in the number of quiver oscillations on the outgoing path. Interferences occur for emission at different times t_i close to different field maxima.

with $\alpha = F_0/\omega^2$, results in a simple relation between the angular momentum L and α,

$$L(k) = (\alpha^2 k^2 + 2\alpha)^{1/2}. \quad (6)$$

This simple *classical* formula allows the prediction of the number of *quantum* interference minima in Fig. 1(c) or the peak in the calculated partial waves populations in Fig. 3. More remarkably, while our calculation pertains to hydrogen we found that the prediction of Eq. (6) agrees also with data for Ar [see [5,27,28]]. In this case the potential of the core is not purely Coulombic. The agreement can be easily explained by the fact that after tunneling, the continuum electron propagates at large distances from the nucleus where the combined laser and asymptotic Coulomb fields dominate. The influence of the core potential is therefore only of minor importance. The initial conditions for the laser-driven trajectory are provided by tunneling ionization with the release of the electron with zero longitudinal velocity at times t_i near the maxima of the field amplitude $F(t_i) \simeq F_0$. Note that the number of quiver oscillations along the Kepler orbit is not unique, thus allowing for path interferences. Figures 4(c) and 4(d) illustrate two examples of such trajectories. Trajectories released at different times t_i or different maxima of the field reaching the same asymptotic branch of the Kepler hyperbola will interfere and generate GRT fringes. In order to reach the limiting case of the dominance of a single P_{l_0}, it is necessary that interference trajectories at fixed energy exist that approximately cover the entire range of scattering angles ($0 \lesssim \theta_k \lesssim \pi$), all of which with angular momenta close to l_0 [Fig. 4(b)]. Our CTMC-T calculations show that close to threshold ($k \lesssim 0.2$) such families of trajectories indeed exist.

In conclusion, we have shown that single ionization of hydrogen by a moderately strong ultrashort laser pulse, in the transition regime from multiphoton to tunneling ionization, gives rise to a complex interference pattern in the two-dimensional momentum (k_z, k_ρ) plane. While at high momenta remnants of ATI rings remain visible, at small k near threshold Ramsauer-Townsend diffraction oscillations develop at fixed k as a function of the angle between emission direction and laser polarization. A simple semiclassical analysis identifies the fringes resulting from interfering paths released at different times but reaching the same Kepler asymptote. The present result shows that a proper semiclassical description along the lines of the ''simple man's model'' [29] requires a three-dimensional description to account for Coulomb scattering. Our results feature a striking similarity to recent data by Rudenko *et al.* [5] suggesting the presence of the 2D interference fringes to be only weakly dependent on the specific atomic core potential.

The authors acknowledge support by the SFB 016 ADLIS, by Project No. P15025-N08 of the FWF (Austria), and by EU Project No. HPRI-2001-50036, and are grateful to A. Rudenko, J. Ullrich, and Lew Cocke for exchanging data.

*Also at: Institute for Astronomy and Space Physics, IAFE, CC 67 Suc. 28, 1428 Buenos Aires, Argentina. Electronic address: diego@iafe.uba.ar

†Also at: Physics Department, Faculty of Applied Mathematics and Physics, National Technical University, Athens, Greece.

[1] G. G. Paulus *et al.*, Nature (London) **414**, 182 (2001); T. Brabec and F. Krausz, Rev. Mod. Phys. **72**, 545 (2000).
[2] A. Baltuska *et al.*, Nature (London) **421**, 611 (2003).
[3] G. G. Paulus *et al.*, Phys. Rev. Lett. **91**, 253004 (2003).
[4] F. Lindner *et al.*, Phys. Rev. Lett.**95**, 040401 (2005).
[5] A. Rudenko *et al.*, J. Phys. B **37**, L407 (2004).
[6] A. Rudenko *et al.*, Phys. Rev. Lett. **93**, 253001 (2004); Th. Weber *et al.*, Phys. Rev. Lett. **84**, 443 (2000).
[7] R. Moshammer *et al.*, Phys. Rev. Lett. **91**, 113002 (2003).
[8] J. Chen, J. Liu, L. B. Fu, and W. M. Zheng, Phys. Rev. A **63**, 011404(R) (2001).
[9] K. I. Dimitriou, D. G. Arbó, S. Yoshida, E. Persson, and J. Burgdörfer, Phys. Rev. A **70**, 061401(R) (2004).
[10] F. H. M. Faisal and J. Schlegel, J. Phys. B **38**, L223 (2005).
[11] A. Rudenko *et al.*, J. Phys. B **38**, L191 (2005).
[12] D. Comtois *et al.*, J. Phys. B **38**, 1923 (2005).
[13] A. de Bohan, Ph.D. thesis, Université Catholique de Louvain, 2001.
[14] S. Dionissopoulou, T. Mercouris, A. Lyras, and C. A. Nicolaides, Phys. Rev. A **55**, 4397 (1997).
[15] J. Wassaf, V. Veniard, R. Taieb, and A. Maquet, Phys. Rev. A **67**, 053405 (2003).
[16] Gerd van de Sand and Jan M. Rost, Phys. Rev. A **62**, 053403 (2000).
[17] D. B. Milosevic, G. G. Paulus, and W. Becker, Opt. Express **11**, 1418 (2003).
[18] P. A. Macri, J. E. Miraglia, and M. S. Gravielle, J. Opt. Soc. Am. B **20**, 1801 (2003).
[19] V. D. Rodriguez, E. Cormier, and R. Gayet, Phys. Rev. A **69**, 053402 (2004).
[20] J. S. Cohen, Phys. Rev. A **64**, 043412 (2001); **68**, 033409 (2003).
[21] X.-M. Tong and S. I. Chu, Chem. Phys. **217**, 119 (1997).
[22] See, e.g., J. J. Barton and D. A. Shirley, Phys. Rev. B **32**, 1892 (1985), and references therein.
[23] W. F. Egelhoff, Phys. Rev. Lett. **71**, 2883 (1993).
[24] J. Burgdörfer, C. Reinhold, J. Sternberg, and J. Wang, Phys. Rev. A **51**, 1248 (1995).
[25] K. J. Schafer and K. C. Kulander, Phys. Rev. A **42**, 5794 (1990).
[26] L. D. Landau and E. M. Lifshitz, *Mechanics* (Pergamon, New York, 1960).
[27] C. M. Maharjan, A. S. Alnaser, I. Litvinyuk, P. Ranitovic, and C. L. Cocke, J. Phys. B **39**, 1955 (2006).
[28] R. Wiehle, B. Witzel, V. Schyja, H. Helm, and E. Cormier, J. Mod. Opt. **50**, 451 (2003).
[29] P. B. Corkum, N. H. Burnett, and F. Brunel, Phys. Rev. Lett. **62**, 1259 (1989); P. B.Corkum, Phys. Rev. Lett. **71**, 1994 (1993); P. B. Corkum, N. H. Burnett, and M. Y. Ivanov, Opt. Lett. **19**, 1870 (1994); M. Ivanov, P. B. Corkum, T. Zuo, and A. Bandrauk, Phys. Rev. Lett. **74**, 2933 (1995).